SEEDED, CONTAINERLESS SOLIDIFICATION OF INDIUM ANTIMONIDE

(Skylab Experiment M-560)*

By

H. U. Walter
The University of Alabama in Huntsville, Department of Physics
Huntsville, Alabama 35807

SUMMARY

Directional solidification of a containerless melt that was suspended at the end of a seed crystal was employed to produce crystals of InSb during Skylab missions(SL3 and SL4).

Single crystals with well developed growth facets ({110}, {111}, {$\bar{1}\bar{1}\bar{1}$}) were obtained. Analysis by X-ray topography and chemical etching shows that the crystals are of high structural perfection. Virtually no dislocation clusters were observed; average dislocation density is of the order of $10^2/cm^2$. The density of dislocations decreases linearly in the center section of space-grown crystals.

A sample that was heavily doped with selenium ($N \approx 10^{19}/cc$) appears to be homogeneously doped in the center section only. Striated solute distribution is observed in the first and the last portion of the space-grown crystal.

*This work was supported by NASA under Contract NAS8-28304.

INTRODUCTION

One of the major attractions of space for processing of materials from the melt is the possibility of handling large quantities of molten materials without the use of containers. This possibility is particularly attractive for highly reactive and high melting temperature materials.

Since gravity-driven convection, which is the major factor that limits the control of directional solidification processes, is lacking as well, space should provide an ideal environment for materials processing from the melt. Provided that second-order effects such as surface tension gradient driven convection are negligible or can be controlled, steep temperature gradients could be established without generating fluid flow. Consequently, unidirectional, steady-state solidification could be achieved. Incorporation of dopant could be controlled perfectly and problems stemming from constitutional supercooling could be overcome.

It can be assumed, however, that for a given material, a practical upper limit for thermal gradients exists. Above this limit, convection driven by surface tension gradients would create similarly uncontrolled conditions as gravity-driven convection does on earth. After initial studies on the feasibility of containerless processing, these limits will have to be investigated and established.

The present study on "Seeded, Containerless Solidification of InSb"* (Skylab Experiment M-560) deals with some of the basic aspects of containerless crystal growth. The objectives of the investigation were defined as follows:

(1) Investigate the feasibility of containerless processing of single crystals in space environment.

(2) Obtain information on the structural perfection of space-grown crystals as compared to samples grown on earth.

(3) Demonstrate the potential of space for producing homogeneously-doped semiconductor material.

---

* This study was initially proposed for germanium; proper melting and temperature gradients could not be established with the existing furnace and it was consequently changed to the lower melting InSb.

EXPERIMENTAL APPROACH AND ARRANGEMENT

A multipurpose electric furnace (M-518) was provided by NASA.* Maximum furnace temperature was 1000°C. Three experiment chambers that could be loaded with different sets of sample cartridges allowed for simultaneous processing of three samples at identical thermal conditions. Each experiment chamber, which is 2.14 cm I.D. and 25 cm deep, has three temperature zones: a 5 cm hot zone in a graphite heat leveler, a 6.3 cm gradient zone, and a heat extraction region of approximately 14 cm. Active control of the heated section of this gradient furnace was provided; the temperature profiles in the samples were determined by the heat-flow characteristics of the sample and sample container.

The basic experimental approach can be described as follows: An oriented, cylindrical single crystal of InSb is mounted into a graphite base that is located at the cold end of the gradient furnace. From this support, the sample extends through the gradient section of the furnace into a hemispherical heating cavity that is located in the hot zone of the furnace. As the graphite cavity is heated, a temperature gradient is established along the crystal, and the sample slowly melts back starting at the bottom of the graphite cavity. The melt adheres to the end of the seed crystal and detaches from the graphite. A spherical melt that is suspended at the end of the seed crystal is formed in the gradient region. During soak, the melt will homogenize; inclusions will partly be accumulated at the surface of the melt and static conditions will be established. During cool down, the seed crystal will grow according to temperature gradients into the containerless melt, and a single crystal will eventually be formed.

The design of the ampoule is shown in Fig. 1. Only high purity materials were used; a major design consideration was to avoid possible contamination of the samples and degradation of materials during the period of approximately 1 year from delivery of ampoules to return of processed samples.

The outer quartz envelope was manufactured from precision-drawn (i.d. = 18 mm $\pm$ 0.025 mm) and precision-ground (0.789 $\pm$ 0.001") clear fused quartz tubing. Single crystals of InSb were grown by the Czochralski technique. Prior to seal off, the ampoules were evacuated to 10^{-9} torr. Ultrahigh purity hydrogen was then admitted to 350 torr and the ampoules were sealed off.

Thermal testing had the objective to establish furnace settings to obtain reproducible meltback of 13 $\pm$ 3 mm as measured from the bottom of the heating cavity.

---

* Design, construction and testing by Westinghouse Electric Corp. under NASA contract.

Furnace settings were established for flight as follows:

Heat leveler temperature	$653^{\circ}C \pm 8^{\circ}C$
Soak time	60 min.
Cool-down rate	$0.6^{\circ}C$/min.

Interface position of 13 mm ± 3 mm and growth rates of 1 - 3 cm/h were expected with these settings.

RESULTS AND DISCUSSION

I. Morphology of Space-Grown Samples

Two sets of cartridges were processed during Skylab missions SL3 and SL4. All cartridges were returned undamaged. With both sets of experiments, recommended soak temperature ($653^{\circ}C \pm 8^{\circ}C$), soak time (1 hr.), and cool-down rate ($0.6^{\circ}C$/min) were met. A temperature versus time plot for two thermocouples, one located in the hot zone, the other in the heat extraction region of the furnace is given in Fig. 2. The upper curve, which represents temperatures measured in the graphite heat leveler at the hot zone of the furnace, indicates constant temperature at $657^{\circ}C$ (printout) for 1 hour. This period is followed by a linear cool-down of $0.6^{\circ}C$/min.

X-ray shadowgraphs of SL3 samples taken prior to opening are shown in Fig. 3. For comparison, a shadowgraph of a sample that was processed on the ground is shown in Fig. 4. Samples processed during SL4 mission show similar silhouettes. Meltbacks of 17.5 mm (E1), 16 mm (D2), 16.5 (D1), 16 mm (D3), 16.5 mm (E3), 16 mm (E2) were obtained as compared to a desired 13 mm ± 3 mm.

Overall views of two representative samples processed during SL3 and SL4 missions are given in Fig. 5 and Fig. 6. Prior to more sophisticated analysis of structural perfection of the samples, single crystallinity could be assessed due to the following reasons: (1) As determined by optical reflection goniometry, well-developed growth facets agree with the crystallographic symmetry of the samples, (2) Single crystal Laue diffraction patterns were obtained, (3) With the exception of two samples (E1 and E3), no grain boundary grooving could be observed. Grooving in the two samples could later be related to a twin-boundary parallel to $\{\bar{1}\bar{1}\bar{1}\}$ which could be traced into the seed; the second twin boundary, apparently (211), was initiated at the periphery of the sample. The generation of this boundary appears to be related to oxide specks that were accumulated at the surface in this area.

An EREP maneuver that was conducted during solidification of SL3 samples (see Fig. 2) apparently caused a disturbance of growth that left a distinct ring-shaped mark on all of the SL3 samples

(see Fig. 5). This time mark in conjunction with the time where cool-down was initiated allows determination of an average growth rate as follows: D1: 10.4 mm/hour, D2: 12.8 mm/hour, E1: 13mm/hour, Since identical furnace settings were used on SL4, an average growth rate of 12 mm/hour can realistically be assumed for SL4 samples.

The general shape of the crystals implies that the melt did adhere to the graphite of the heating cavity instead of being freely suspended at the end of the seed crystal. A teardrop-shaped melt was, therefore, formed that was supported at one end of the seed and that was attached to the bottom of the heating cavity at the other end. The small protrusion at the end of the crystal can be explained by the fact that InSb expands by approximately 11% upon solidification; directional solidification would consequently result in a small amount of melt having to escape when the solidifying crystal meets the bottom of the heating cavity.

Contact angles of InSb at 530°C to 550°C on graphite substrates prepared from the same material and having comparable surface finish as the graphite cavity were determined by sessile-drop methods as $130^{\circ} \pm 3^{\circ}$. No hysteresis could be observed. Since the shape of liquids is determined by minima of free surface energy, a situation where the melt is attached to the seed as well as to the bottom of the graphite heating cavity is energetically instable.

Alternatively, directional solidification of a spherical melt that is suspended at the end of a cylindrical seed crystal can be described as follows: In the most simple case, no volume changes are involved with the transition from liquid to solid, and the surface of the solid follows the surface of the liquid which meets the solid surface tangentially at all times during solidification. The resulting solid will be a true replica of the melt. If volume changes are considered, different shapes of the solid will result. In the case of expansion, elongated, bulb-shaped samples will be formed; in case of contraction, a geoid shape with flattened end will result.

Since as a rule little change of volume is observed in the melting process of metals (only about 3% or less), replicas of melt shapes are obtained. Our early experimentation had been confined to solidification of metals[1,2] and the initial title of the experiment "spherical crystals" stems from this.

With germanium, where an increase in volume of about 5% is associated with solidification, nonspherical shapes are observed. Samples prepared by directional solidification of sessile drops of germanium with solidification starting from the base, have characteristic onion shapes; a behaviour that has been observed previously.[3]

The next complication that can be added to this model is that the surface of the growing solid does not follow the shape of the liquid. Instead, a situation exists as shown in Fig. 7a and 7b, where the meniscus of the liquid meets the solid at an angle. As shown in Fig. 7c and 7d, upper and lower limits for this angle can be introduced. Angles higher or lower than this limit would represent an instable wetting situation where surface breakdown and rearrangement would result. Evidence from space-grown crystals supports this model of free solidification.

Extremely well-developed {110} facets, generally more disturbed {111} facets and small {211} facets are observed. Six {110}* facets ($1\bar{1}0$, $10\bar{1}$, $01\bar{1}$, $\bar{1}10$, $\bar{1}01$, $0\bar{1}1$) are parallel to the [111] growth direction. Similar to the example given in Fig. 7a, these facets are primarily responsible for the rather prismatic shape of the samples. Three $\{\bar{1}\bar{1}\bar{1}\}$ facets ($11\bar{1}$, $\bar{1}11$, $1\bar{1}1$) and three {111} facets ($1\bar{1}\bar{1}$, $\bar{1}1\bar{1}$, $\bar{1}\bar{1}1$) are inclined $19^{\circ}28'$ to the direction of growth. {111} facets which are terminated with Sb atoms would grow away from the seed axis, the $\{\bar{1}\bar{1}\bar{1}\}$ would grow toward the seed. With the facet growing into the melt as with $\{\bar{1}\bar{1}\bar{1}\}$, a situation should be created similar to the one shown in Fig. 7c, where the facet becomes instable and growth is periodically interrupted. Terracing caused by periodic surface breakdown can indeed be observed on $\{\bar{1}\bar{1}\bar{1}\}$ facets.

Facets are observed with crystals grown on the ground as well. Facets on the space-grown samples are, however, generally less disturbed. Aside from hillocks and scattered pits, facets of undoped crystals are exceptionally flat.

Hillocks cannot be avoided with InSb; they are formed above $350 - 400^{\circ}C$[5,6] because Sb evaporates preferentially from heated InSb surfaces. At the melting point, partial pressures of In and Sb are 10^{-6} and 10^{-3} mm/g respectively.[7] As a result, indium-rich droplets are formed; these droplets solidify at lower temperatures and appear as hillocks.

Aside from hillocks which would not be found with monocomponent systems such as germanium or silicon, the facets are of remarkable optical quality and flatness. Tolanski multiple-beam interference microscopy (Fig. 8) shows straight and equally-spaced interference fringes. Using the Tolanski microscope with the Fizeau-flat parallel to the surface of the facet (interference contrast), a single dark fringe can be made to cover a complete facet. This latter phonemenon is proof for overall flatness of some facets to a few hundred Å.

---

*Dewalt[4] denomination.

II. Assessment of Structural Perfection and Chemical Homogeneity

The two ruling parameters, composition (stoichiometry, dopant distribution, inclusions, precipitates, etc.) and structure of a crystalline material can be considered separately to a limited extent only. As an example, variation in dopant concentration is associated with variation in lattice parameters, inclusions and precipitates disturb the periodicity of the lattice. Similarly, low defect density and in particular absence of grain boundaries is a prerequisite for electronically useful material as well as chemical homogeneity.

As mentioned above, overall single crystallinity could be verified by optical reflection goniometry and Laue diffraction. As can be expected, all facets are low Miller index planes ({111}, $\{\bar{1}\bar{1}\bar{1}\}$,{110}, {211}).

Reflection X-ray topography[8] (Berg-Barrett geometry) was used to study the structural quality of the crystals prior to cutting or any surface preparation. The experimental arrangement is shown in Fig. 9. The actual apparatus used was a Lang camera that was modified for taking scanning reflection topographs. A standard X-ray tube with copper target was used. The technique can briefly be described as follows: A divergent beam of X-rays is emitted from an X-ray focal spot and passes through a set of slits of defined separation (L_1) onto the crystal. The crystal is set at the appropriate angle to diffract the incoming X-rays into an X-ray counter set at $2\theta_B$, twice the Bragg angle. The counter is used to align the crystal for maximum diffracted intensity. An X-ray sensitive film is inserted between the crystal and X-ray counter and the diffracted beam image is recorded on the film. In order to prevent the direct beam from exposing the film, a second slit system (L_2) is placed between crystal and film. This slit is adjusted to allow passage of only the diffracted beam. L_1 is kept so that the divergence of the primary beam is small enough to allow separation of $K\alpha_1$ and $K\alpha_2$ images. During exposure, film and sample are simultaneously translated so that the X-ray beam slowly scans the surface of the sample, and an image of a larger area of the surface of the crystal is recorded.

Examples of reflection topographs obtained in this manner are shown in Figs. 10, and 11. Symmetrical reflections about [111] and [110] were used to obtain the topographs shown in the figures. One single Bragg reflection is obtained that reflects all of the crystal surface exposed to the X-ray beam. No grain or lattice misorientation can be observed. Geometrical irregularities of the surface show up on the topograph as well; shadows are cast by small oxide specks which can be seen on some of the pictures. Aside from this, the space-grown portion exhibits flawless single crystals. Only at the very end of the space-grown samples, irregularities show up; this is, however, to be expected since this portion was grown under increasing radial thermal gradients and the material was then in contact with the mold.

Etching of dislocations is a well-established procedure with InSb. In particular In-dislocations can reliably be revealed by etching of {111} planes in CP4 etchants. Crystals were cut into thin wafers perpendicular to the axis of growth. In-dislocations in one sample as revealed by etching are shown in Fig. 12. This sample was prepared during SL3 mission; a sample grown during SL4 mission has not yet been investigated.

Dislocation density in the earth-grown seed has a rather wide spread. This scatter seems to be less in the space-grown portion of the crystal. Since the wafers that were etched are presently used for electrical measurements, no additional data points could be taken so far. After the electrical measurements are completed, further step-etching will be done to obtain more data points. Additional dislocations are generated during the initial period of growth; a linear decrease follows and in the last portion of the space-grown crystal, the density increases due to increasing radial temperature gradients. A small maximum seems to appear at the beginning of the last third of the space-grown crystal. This maximum coincides with the perturbation caused by the EREP maneuver; this event is also marked on the surface of the sample as has been mentioned earlier. The dislocation density profile for a second sample (also SL3) shows similar features. Consistent with the sample just described, the density of dislocations decreases rather linearly in the middle section of the space-grown crystal. The density is reduced by a factor of about 6 over a growth distance of 1 cm.

To answer questions concerning redistribution of dopant and convective flow in the melt, one of the samples of the flight set was heavily doped with selenium ($N \approx 10^{19}$/cc). With this sample, three regions where dopant was incorporated in different manners could be discerned. As determined by etching and X-ray topography, no inhomogeneities could be detected so far in the center section of the crystal. The part of the sample that solidified last, shows distinct banding; a wave-like variation of dopant concentration is indicated in X-ray photographs and etched surfaces. An unusual sequence of striations that is also reflected on the surface of the crystal can be observed in the first third of the crystal. Distinct decoration of the interface can be observed; starting from the seed, the spacing increases exponentially; the period then becomes constant and the markings disappear. For conclusive interpretation of this behavior, dopant profiles will have to be determined. It seems, however, that the sequence described could develop only if no appreciable fluid flow would have disturbed the solidification process. This would indicate that not only gravity-driven convection but surface tension gradient-driven convection as well were insignificant.

CONCLUSION

Based on this investigation, the following conclusions concerning containerless processing of single crystals from the melt in low gravity environment can be reached:

(1) Highly perfect single crystals can be prepared by seeded, containerless solidification. For processing of highly reactive materials and high melting temperature materials, the technique described should be especially valuable; large crystals could be prepared by this technique as well.

(2) Even though dopant inhomogeneities are observed, all indication points to essentially no-fluid-flow conditions. Consequently, production of homogeneously doped single crystals by containerless techniques appears to be feasible.

ACKNOWLEDGMENT

This study was only possible with the direct and indirect support given by a large number of persons. The author is indebted to all of them. Special thanks are due to Messrs. W. R. Adams, T. C. Bannister, A. Boese, Dr. J. H. Bredt, M. C. Davidson, R. Fatheree, L. Gibbs, J. Levie, D. P. Nicolas, Dr. R. S. Snyder, Prof. A. F. Witt and J. Zwiener for technical and administrative support as well as for helpful suggestions and interesting and stimulating discussions.

REFERENCES

1. H. U. Walter, R. S. Snyder, J. Less Common Metals, 24 (1971) 467-469.

2. H. U. Walter, J. Crystal Growth, 10 (1971) 309-312.

3. G. A.Kurov, A. I. Petrin, V. V. Ignatev, Sov. Phys. - Crystallography, 14 (1969) 122.

4. K. F. Hulme, J. B. Mullin, Solid State Electronics, Pergamon Press 1962, Vol. 5, 211-247.

5. D. Haneman, J. Appl. Phys., 31 (1960) 217.

6. M. F. Millea, C. T. Tomizuka, J. Appl. Phys., 27 (1956) 96.

7. V. K. Ilin, S. I. Aksenov, Inorganic Materials, 7 (1970) 1114.

8. J. Auleytner, "X-ray Methods in the Study of Defects in Single Crystals," Pergamon Press (1967).

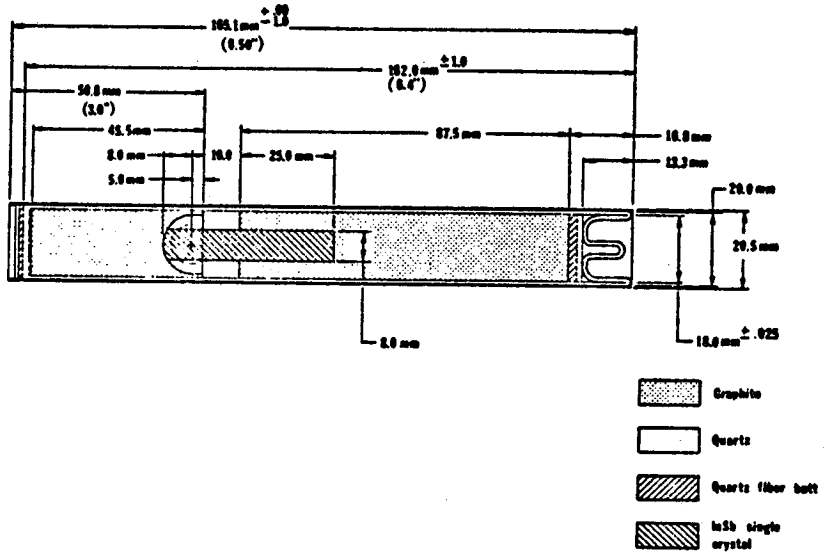

FIGURE 1. AMPOULE DESIGN

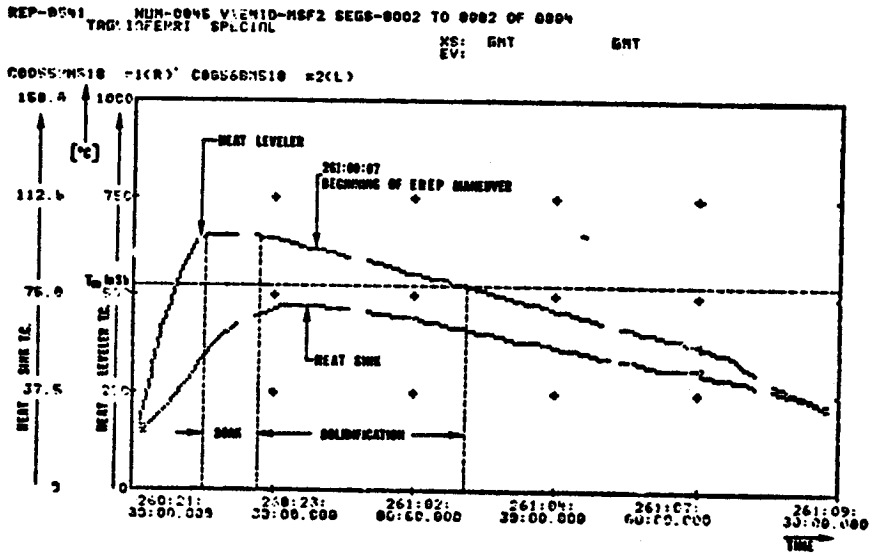

FIGURE 2. HEAT LEVELER AND HEAT SINK TEMPERATURE DURING PROCESSING OF M-560 SAMPLES (SL-3 MISSION)

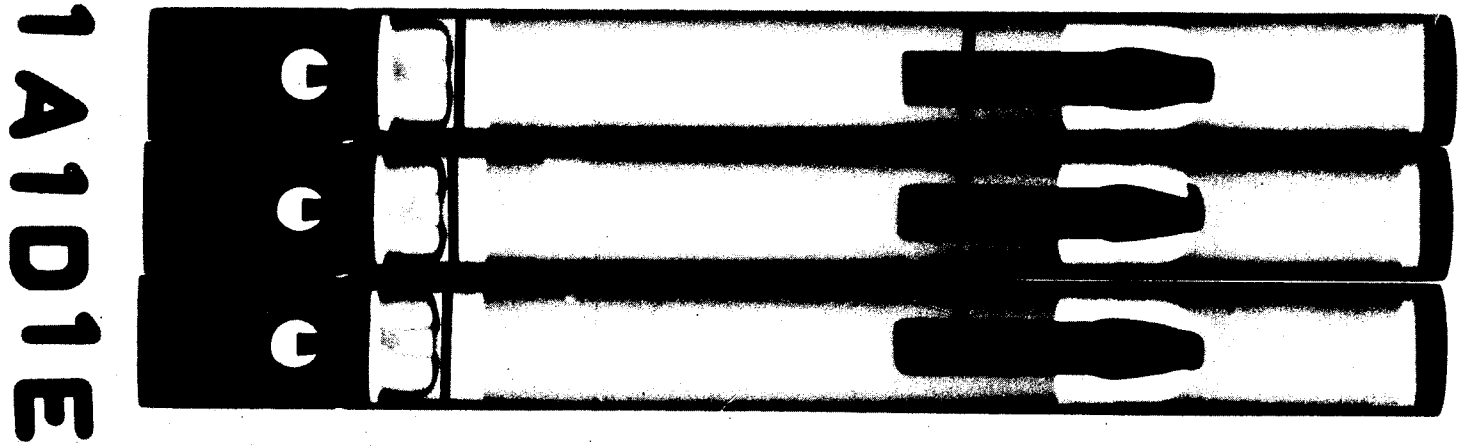

FIGURE 3. X-RAY SHADOWGRAPHS OF CARTRIDGES PRIOR TO OPENING

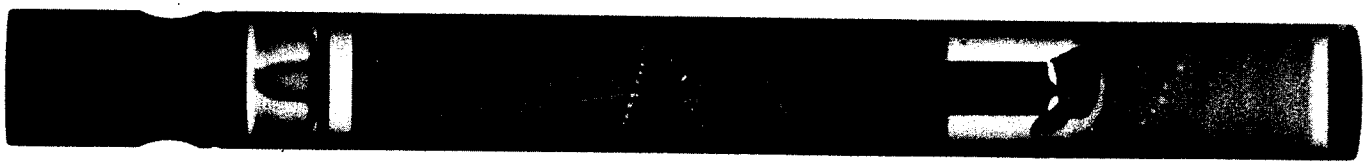

FIGURE 4. X-RAY SHADOWGRAPH OF TEST SAMPLE AFTER THERMAL TESTING

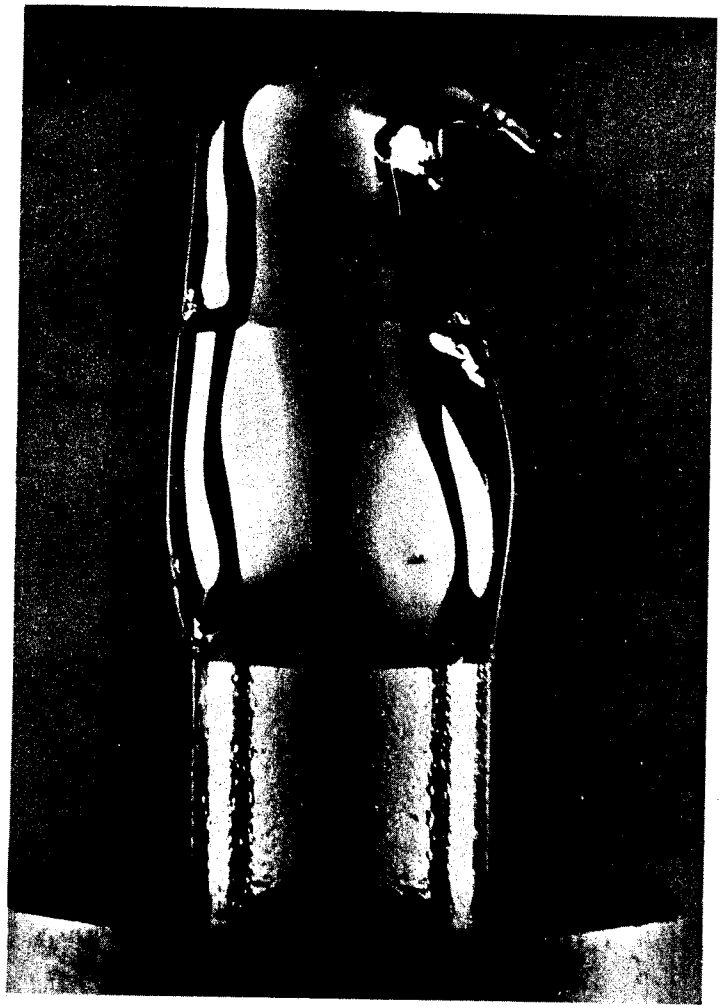

FIGURE 5. SAMPLE PROCESSED DURING SL-3 MISSION

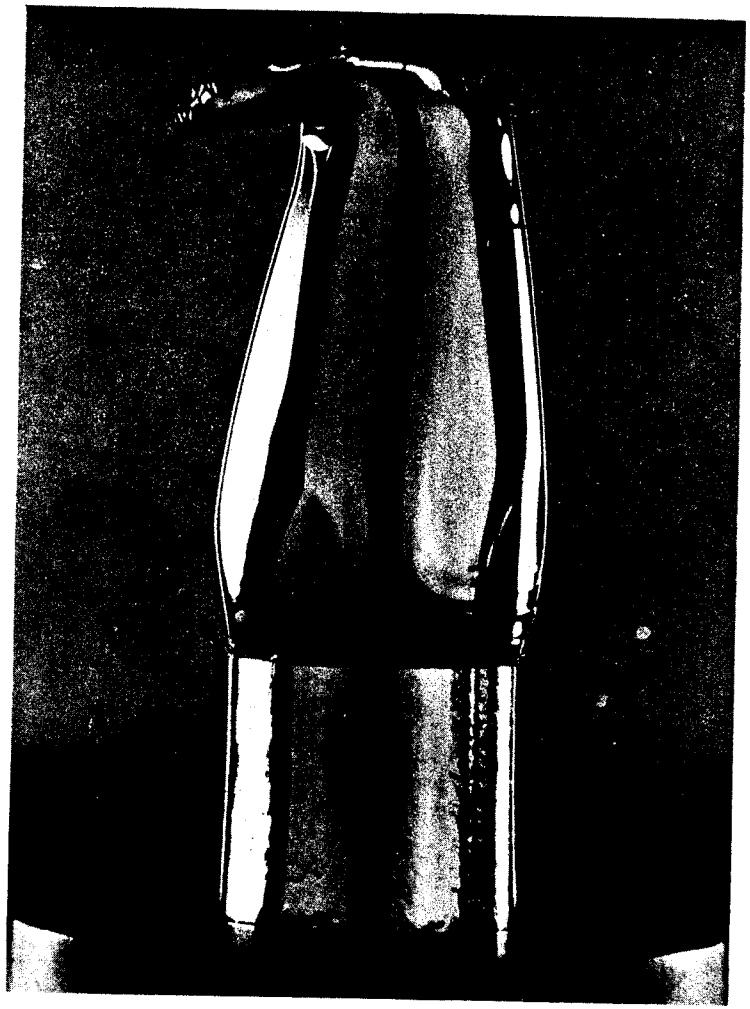

FIGURE 6. SAMPLE PROCESSED DURING SL-4 MISSION

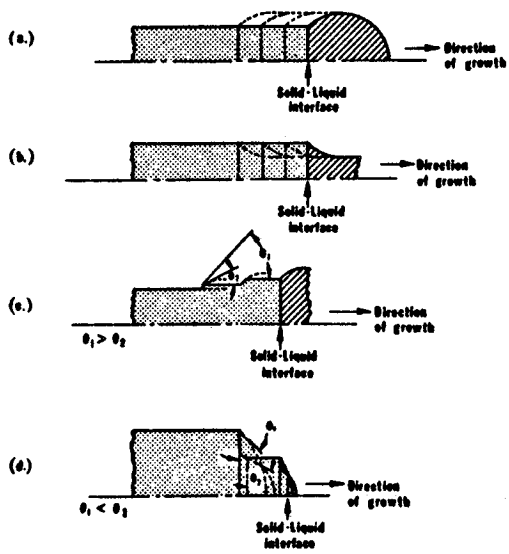

FIGURE 7. DIRECTIONAL SOLIDIFICATION OF DROPS.

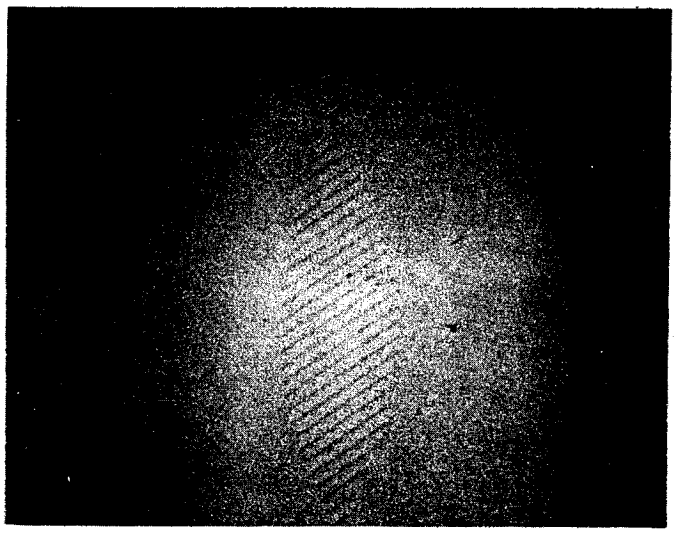

FIGURE 8. TOLANSKI PHOTOGRAPH OF (111) FACET

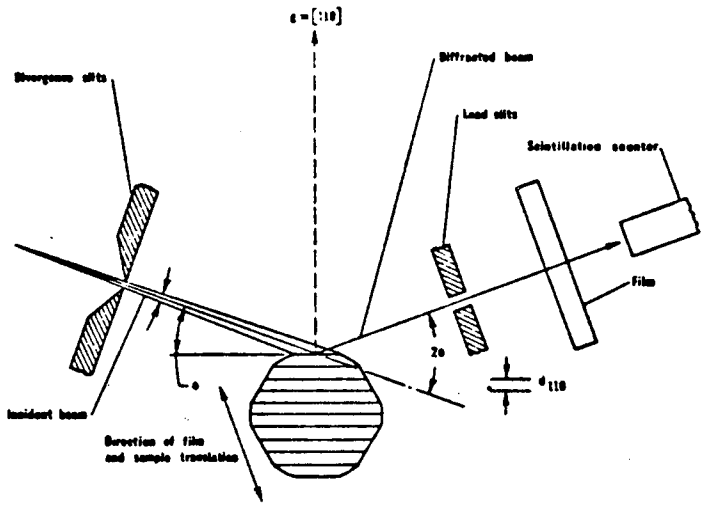

FIGURE 9. SCHEMATIC OF SCANNING REFLECTION TOPOGRAPHY

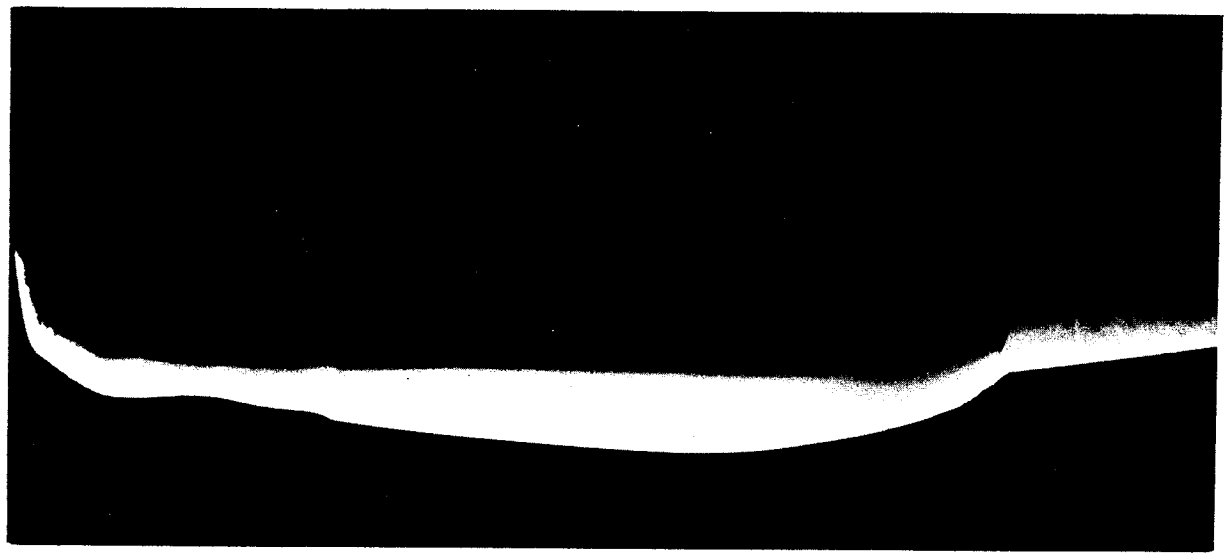

FIGURE 10. SURFACE TOPOGRAPH, (220) REFLECTION.

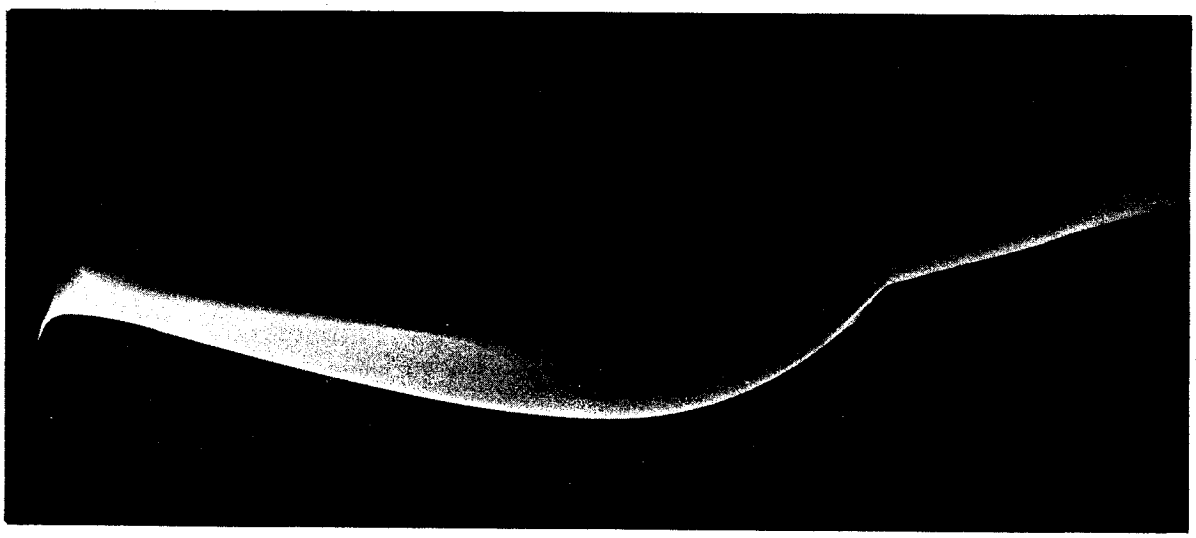

FIGURE 11. SURFACE TOPOGRAPH, (111) REFLECTION

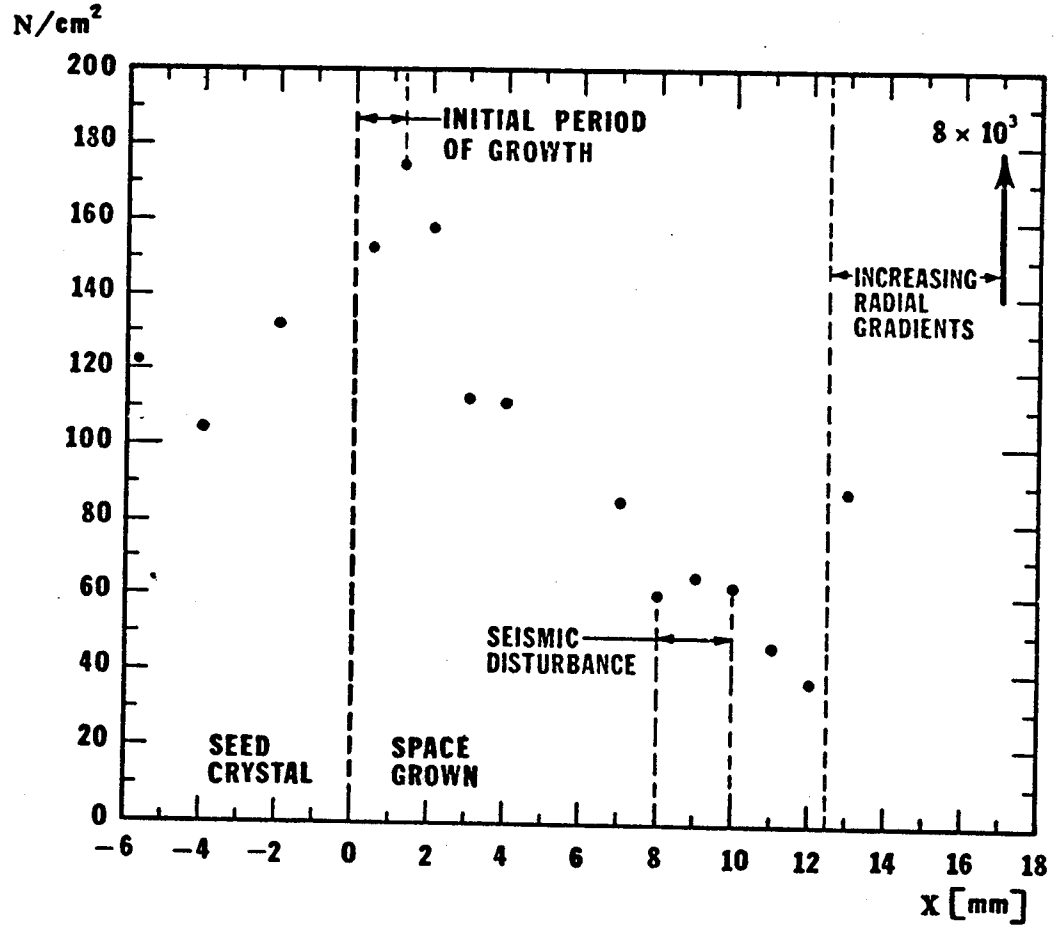

FIGURE 12. INDIUM DISLOCATIONS IN SAMPLE PROCESSED DURING SL-3 MISSION